SCIENCE CHINA
Technological Sciences

January 2012 Vol.55 No.1: 244–254
doi: 10.1007/s11431-011-4663-y

On the treatment of solid boundary in smoothed particle hydrodynamics

LIU MouBin[1,2*], SHAO JiaRu[1] & CHANG JianZhong[3]

[1] *Key Laboratory for Hydrodynamics and Ocean Engineering, Institute of Mechanics, Chinese Academy of Sciences, Beijing 100190, China;*
[2] *State Key Laboratory for Nonlinear Mechanics, Institute of Mechanics, Chinese Academy of Sciences, Beijing 100190, China;*
[3] *School of Mechatronic Engineering, North University of China, Taiyuan 030051, China*

Received April 28, 2011; accepted June 23, 2011; published online November 27, 2011

As a popular meshfree particle method, the smoothed particle hydrodynamics (SPH) has suffered from not being able to directly implement the solid boundary conditions. This influences the SPH approximation accuracy and hinders its further development and application to engineering and scientific problems. In this paper, a coupled dynamic solid boundary treatment (SBT) algorithm has been proposed, after investigating the features of existing SPH SBT algorithms. The novelty of the coupled dynamic SBT algorithm includes a new repulsive force between approaching fluid and solid particles, and a new numerical approximation scheme for estimating field functions of virtual solid particles. The new SBT algorithm has been examined with three numerical examples including a typical dam-break flow, a dam-break flow with a sharp-edged obstacle, and a water entry problem. It is demonstrated that SPH with this coupled dynamic boundary algorithm can lead to accurate results with smooth pressure field, and that the new SBT algorithm is also suitable for complex and even moving solid boundaries.

smoothed particle hydrodynamics (SPH), particle method, solid boundary treatment (SBT), coupled dynamic SBT

Citation: Liu M B, Shao J R, Chang J Z. On the treatment of solid boundary in smoothed particle hydrodynamics. Sci China Tech Sci, 2012, 55: 244–254, doi: 10.1007/s11431-011-4663-y

1 Introduction

Smoothed particle hydrodynamics (SPH) is a popular meshfree, Lagrangian, particle method with some attractive features [1, 2]. It was invented to solve astrophysical problems in three-dimensional open space. In SPH, the state of a system is represented by a set of particles, which possess individual material properties and interact with each other within a certain range defined as the support domain by a weight function or smoothing function [3]. Flow field variables (such as density, velocity, acceleration) can be obtained through approximating the governing equations which are discretized on the set of particles. Compared with traditional grid-based numerical methods, SPH has special advantages. Particles in the SPH method move along with the modeling objects. Therefore, SPH has Lagrangian feature and can naturally obtain time history. By properly deploying particles at specific positions at the initial stage, it is feasible to trace free surfaces, material interfaces, and moving boundaries conveniently in the process of simulation. Also because no grid/mesh is used, the connectivity between particles is generated as part of the computation and can change with time. Therefore SPH allows a straightforward handling of very large deformation. Due to its inherent features and advantages, SPH has been widely applied to different areas in engineering and sciences [4].

However, developments and applications of the SPH method have been hindered by a number of numerical issues. One major problem is associated with the SPH ap-

*Corresponding author (email: liumoubin@imech.ac.cn)

proximation scheme, which is closely related to accuracy, stability, and efficiency. During the past decades, many researchers have been investigating the numerical approximation schemes of SPH, and a number of effective algorithms have been developed [2]. Another major issue is the treatment of solid boundaries and implementation of the solid boundary conditions. In SPH, the obstacle areas and flow regions can both be discretized with particles. Since particles can move with the modeling objects according to internal and external forces, the connectivity between moving particles changes at each time step. This is similar to the classic molecular dynamics (MD) method [5] that uses a particle to represent an atom or a molecule in nano-scale, and the dissipative particle dynamics (DPD) method [6] that uses a particle to represent a small cluster of molecules in meso-scale. In SPH, solid boundary conditions are not able to be directly and rigorously implemented as in the grid-based numerical models. Since its invention, the treatment of solid boundary has been a numerical focus, which has been influencing the accuracy of SPH, and hindering its further development and application in engineering and sciences [7, 8].

In this paper, we investigate the treatment of solid boundary and implementation of solid boundary conditions for the SPH method. The paper is organized as follows. The second section provides a brief overview of the SPH method on modeling incompressible flows. In the third section, existing SBT algorithms are revisited, and classified into three major classes according to their features. After that, a coupled dynamic boundary treatment algorithm is proposed. In Section five, the new SBT algorithm is tested on three numerical examples with detailed analyses and comparison with other approaches. The paper ends in Section six with some concluding remarks.

2 A brief overview of SPH methodology

The conventional SPH method was originally developed for hydrodynamic problems in which the governing equations are in strong form of partial differential equations of field variables such as density, velocity, and etc. There are basically two steps in obtaining an SPH formulation, kernel and particle approximations. The kernel approximation is to represent a function and its derivatives in continuous form as integral representation using the smoothing function and its derivatives. In the particle approximation, the computational domain is discretized with a set of particles. A field function and its derivative can be written in the following forms:

$$\langle f(\boldsymbol{x}_i)\rangle = \sum_{j=1}^{N} \frac{m_j}{\rho_j} f(\boldsymbol{x}_j) W(\boldsymbol{x}_i - \boldsymbol{x}_j, h), \tag{1}$$

$$\langle \nabla f(\boldsymbol{x}_i)\rangle = \sum_{j=1}^{N} \frac{m_j}{\rho_j} f(\boldsymbol{x}_j) \nabla_i W_{ij}, \tag{2}$$

where $\langle f(\boldsymbol{x}_i)\rangle$ is the approximate value of particle i, $f(\boldsymbol{x}_j)$ is the value of $f(\boldsymbol{x})$ associated with particle j, $\boldsymbol{x}_i$ and $\boldsymbol{x}_j$ are the positions of corresponding particles, h is the smooth length, N is the number of the particles in the support domain, W is the smoothing function and represents a weighted contribution of particle j to particle i.

Using eqs. (1) and (2) with necessary numerical tricks, it is possible to derive SPH formulations for partial differential equations governing the physics of fluid flows. For example, the Navier-Stokes (NS) equations, which control the general fluid dynamic problems, can be written in the following forms:

$$\frac{\mathrm{d}\rho}{\mathrm{d}t} = -\rho \nabla \cdot \boldsymbol{v}, \tag{3}$$

$$\frac{\mathrm{d}\boldsymbol{v}}{\mathrm{d}t} = -\frac{1}{\rho}\nabla p + \frac{\mu}{\rho}\nabla^2 \boldsymbol{v} + \boldsymbol{g}, \tag{4}$$

where ρ, v, p, $\boldsymbol{g}$ and μ denote density, velocity vector, pressure, gravity and dynamic viscosity, respectively. By substituting the SPH approximations for a function and its derivative to NS equations, the SPH equations of motion for NS equations can be obtained as

$$\frac{\mathrm{d}\rho_i}{\mathrm{d}t} = \sum_{j=1}^{N} m_j \boldsymbol{v}_{ij} \cdot \nabla_i W_{ij}, \tag{5}$$

$$\frac{\mathrm{d}\boldsymbol{v}_i}{\mathrm{d}t} = -\sum_{j=1}^{N} m_j \left(\frac{p_i}{\rho_i^2} + \frac{p_j}{\rho_j^2} \right) \nabla_i W_{ij} + \sum_{j=1}^{N} \frac{4 m_j \left(\mu_i + \mu_j\right) \boldsymbol{x}_{ij} \cdot \nabla_i W_{ij}}{\left(\rho_i + \rho_j\right)^2 \left(x_{ij}^2 + 0.01h^2\right)} \boldsymbol{v}_{ij} + \boldsymbol{g}. \tag{6}$$

In SPH, an artificial compressibility technique is often used to model an incompressible flow as a slightly compressible one. The artificial compressibility considers that every theoretically incompressible fluid is actually compressible. Therefore, it is feasible to use a quasi-incompressible equation of state to model the incompressible flow. In this work, the artificial equation of state is

$$p = c^2 \rho, \tag{7}$$

where c is the sound speed of the concerned artificially compressible fluid (e.g. water). Monaghan [9] argued that the relative density variation, δ, is related to the fluid bulk velocity and sound speed in the following way

$$\delta = \frac{\Delta\rho}{\rho_0} = \frac{\left|\rho - \rho_0\right|}{\rho_0} = \frac{\boldsymbol{v}_b^2}{c^2} = M^2, \tag{8}$$

where ρ_0, $\Delta\rho$, $\boldsymbol{v}_b$ and M are the initial density, absolute density variation, fluid bulk velocity and Mach number, respectively.

Morris [10], through considering the balance of pressure, viscous force and body force, proposed an estimation of

sound speed. He argued that the square of the sound speed should be comparable with the largest value of V_b^2/δ, $\upsilon V_b/\delta l$, and Fl/δ, i.e.,

$$c^2 = \max\left(\frac{V_b^2}{\delta}, \frac{\upsilon V_b}{\delta l}, \frac{Fl}{\delta}\right), \tag{9}$$

where υ ($\upsilon=\mu/\rho$) is the kinetic viscosity, F is the magnitude of the external body force, and l is the characteristic length scale.

Except for artificial compressibility, artificial viscosity [11], kernel gradient correct (KGC) model, and RANS turbulence model [12] are used in this paper to model incompressible fluid flows. The KGC model can guarantee second order accuracy of the kernel gradient approximation, while the RANS model is used to describe the inherent turbulence effects.

SPH method uses artificial viscosity frequently in modeling shock wave problems such as explosion and impact. Artificial viscosity can diffuse sharp variations and dissipate energy of high frequency terms. The Monaghan type artificial viscosity is frequently used, which consists of a linear term and a quadratic term with both coefficients approximately equal to 1.0. It can effectively resolve shock waves within several smoothing lengths. On the other hand, the artificial viscosity helps to regularize particle distribution, remove numerical oscillation and instability. In modeling incompressible free surface flow problems, the physical viscosity rather than artificial viscosity should be used. However, we found that incompressible free surface flow usually generates irregularly distributed particles locally, while an artificial viscosity with only the linear term can help to effectively remove particle irregularity. According to our experience, an optimal range of the coefficient of the artificial viscosity linear term is around 0.05–0.1. In this paper, the coefficient is taken as 0.08.

3 Solid boundary treatment

To well implement the solid boundary conditions and improve the numerical accuracy, many researchers have proposed different SBT algorithms for the SPH method. Except for approaches with coupled grid-based methods, which can take the advantages in dealing with solid boundaries, most SBT algorithms use virtual particles (or ghost or image particles in different references) to represent the solid boundary (and even the solid obstacle areas). Depending on the deployment of the virtual particles and numerical approximation schemes to obtain field variables of the corresponding virtual particles, these SBT algorithms can be classified into three major classes: repulsive force SBT, dynamic SBT and conventional SBT algorithms with ghost particles. In this section, a detailed analysis of these three classes of SBT algorithms will be conducted first, and then a coupled dynamic SBT algorithm will be proposed, which intends to take the full advantages of the existing algorithms while removing their disadvantages.

3.1 Repulsive force SBT algorithm

The repulsive force SBT algorithm was first presented by Monaghan [13] who used a line of virtual particles (as repulsive particles) located right on the solid boundary to produce a highly repulsive force on the approaching fluid particles near the boundary, and thus to prevent these fluid particles from unphysical penetration through solid boundaries, as shown in Figure 1.

The early repulsive force is very much similar to the Lennard-Jones (LJ) form molecular force in classic molecular dynamics, which can be written as follows:

$$PB_{ij} = \begin{cases} D\left[\left(\dfrac{r_0}{r_{ij}}\right)^{n_1} - \left(\dfrac{r_0}{r_{ij}}\right)^{n_2}\right]\dfrac{x_{ij}}{r_{ij}^{\ 2}}, & \left(\dfrac{r_0}{r_{ij}}\right) \leqslant 1, \\ 0, & \left(\dfrac{r_0}{r_{ij}}\right) > 1, \end{cases} \tag{10}$$

where PB_{ij} and r_{ij} are the repulsive force and distance between a solid particle and an approaching fluid particle, respectively. Parameters n_1 and n_2 are usually taken as 12 and 4, respectively. r_0 is the cut-off distance. D is a problem dependent parameter, and should be chosen to be in the same scale as the square of the largest velocity. It is clear that the LJ form force is highly repulsive and approaches infinite when the two particles approaches. The force is sensitive to parameters such as n_1, n_2, r_0 and D. For example, if the cutoff distance r_0 is too large, some fluid particles may feel early and unnecessary repulsive force. This leads to initial disturbance and even blowup of fluid particles. If r_0 is too small, fluid particles may have already penetrated the boundary before experiencing repulsive force. In most practices, r_0 is usually close to the initial particle spacing.

An improved repulsive model was given by Rogers and Dalrymple [14] in modeling tsunami waves and runup as

$$\overline{f} = \boldsymbol{n} R(\phi) P(\varphi) \varepsilon(z, u_\perp), \tag{11}$$

where $\boldsymbol{n}$ is the normal direction of the solid boundary, ϕ is the perpendicular distance between the two particles, φ is the projection of interpolation location φ_i onto the chord , $u_\perp$ is the normal velocity of the fluid particles, and z is the elevation above the local still water level. $R(\phi)$ is a finite, repulsive function related to the positions of the two particles. It is obvious that except for distance, normal and tangential

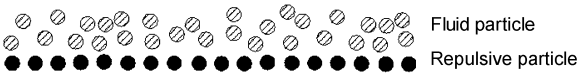

Figure 1 Illustration of the repulsive force SBT algorithm.

directions are necessary to be determined before calculating the repulsive force.

3.2 Dynamic SBT algorithms

In dynamic SBT algorithms, virtual particles are placed and fixed in the boundary area, and the thickness of the virtual boundary particles is related to the kernel function as well as initial particle spacing (see Figure 2). Virtual particles are used to approximate the field variables of fluid particles, and thus to improve the SPH numerical accuracy near boundary areas through removing the boundary deficiency problem. On the other hand, the field variable of the virtual particles can be obtained from SPH approximation on governing equations such as the continuity equation, momentum equation and the equation of state. Since field variables of the virtual particles are dynamically evolved according to the governing equations, the involved solid boundary treatment is usually referred to as dynamic SBT.

The idea of dynamic boundary treatment was mentioned in Liu and Liu's SPH monograph [11], and was successfully implemented by Dalrymple and his co-workers in modeling free surface flows [15]. In approximating field variables of virtual particles, numerical problems with boundary deficiency still exist. As for a concerned virtual particle, there are not sufficient particles in its support domain to take part in the weighted summation process. Therefore, the dynamic SBT algorithm can also lead to inaccurate results with pressure oscillations. Gong and Liu [16] proposed an improvement in smoothing the pressure field in their dynamic SBT algorithm, and it is reported to have better performance, especially in removing pressure oscillations.

3.3 Conventional SBT algorithms with ghost particles

Conventional SBT algorithms with ghost particles have been frequently used in SPH. In this method, ghost particles are generated to represent the solid boundary areas by mirroring or reflecting fluid particles along solid boundaries (Figure 3). A line of boundary particles may also be used to exert repulsive forces. Ghost particles can be generated only once at the first time step, and fixed in the computational domain for later approximations. They can also be generated at each time step and adapt to changing neighbor fluid particles. Ghost particles can take part in the SPH approximation process of the fluid particles to improve boundary accuracy, while different ways to obtain the field variables can lead to different implementations.

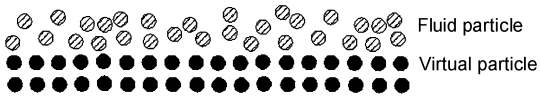

Figure 2 Illustration of the dynamic SBT algorithm.

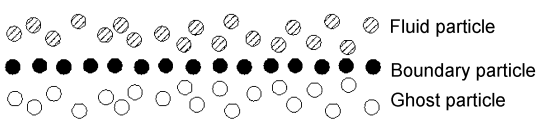

Figure 3 Illustration of the conventional SBT algorithm with ghost particles.

Libersky and his co-workers [17] introduced ghost particles to reflect a symmetrical surface boundary condition with opposite velocity on the reflecting image particles. Colagrossi [18] used an approach to mimic the solid boundary by ghost particle with density, pressure and velocity from neighbor fluid particles. For the free-slip condition, for example, flow variables of ghost particles can be written as

$$\begin{cases} x_g = 2x_w - x_i, \quad y_g = 2y_w - y_i, \\ v_{g,t} = v_{i,t}, \quad v_{g,n} = -v_{i,n}, \\ p_g = p_i, \quad \rho_g = \rho_i, \end{cases} \tag{12}$$

where subscript i refers to the fluid particle, g refers to the ghost particle, and w is the corresponding wall particle. $v_{g,t}$ and $v_{i,t}$ are the tangential velocities of the ghost particle and the fluid particle, and $v_{g,n}$ and $v_{i,n}$ are the normal velocities. For non-slip boundary conditions, both tangential and normal velocities are reversed.

Morris et al. [10] proposed an approach to obtain velocity of virtual boundary particles for implementing non-slip boundary conditions. Particles are created on a regular lattice, and contribute to the computation of the density and pressure gradients of fluid particles. The velocities of the boundary particles are obtained through the ratios of the distances from real particles and boundary particles to the boundary, as shown in Figure 4.

The relative velocity between the two kinds of particles can be obtained using the following equations:

$$V_{ab} = \beta V_a, \tag{13}$$

$$\beta = \min(\beta_{\max}, 1 + d_B / d_a), \tag{14}$$

where d_a and d_B are the normal distances between the real particle A and ghost particle B to the solid boundary, V_{ab} is the relative velocity, and $\beta_{\max}$=1.5.

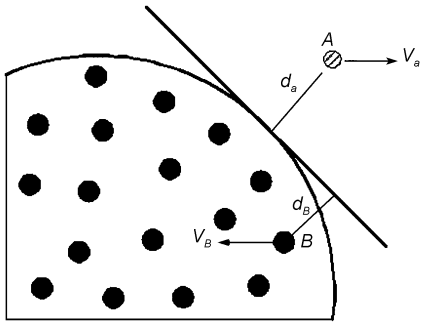

Figure 4 Illustration of the improved ghost particle SBT algorithm by Morris et al. [10].

Marrone et al. [19] proposed an improved SBT algorithm with fixed ghost particle and used it to simulate dam break problems. The solid boundary is represented by several layers of fixed ghost particles. To obtain variables (such as density, pressure and velocity) of a fixed ghost particle, it is necessary to introduce an image interpolation point (hollow triangle in Figure 5) by reflecting a concerned ghost particle (filled triangle in Figure 5) to the flow region. The field variables of the image interpolation point can be obtained from traditional SPH approximating or enhanced SPH approximating such as the MLS method [20] over neighbor particles, and can be used as the variables of a fixed ghost particle. It is reported that this SBT algorithm can lead to good numerical accuracy with smooth pressure distribution.

3.4 Remarks and discussions

A good solid boundary treatment algorithm should take care of accuracy, efficiency as well as adaptivity to complex boundaries. It is clear that the repulsive force solid boundary treatment is conceptually simple, easy to implement, and adaptive to complex solid boundaries. However, the numerical accuracy is poor due to serious boundary deficiency problem as there are no sufficient neighbor particles for a fluid particle near the solid boundaries. Also the numerical accuracy is usually sensitive to the coefficients of the specific repulsive force. For example, the frequently used LJ form repulsive force is effective in preventing fluid particles from penetrating solid walls, but it may lead to rough pressure field, and even unphysical separation of fluid particles away from the solid wall. The soft repulsive force model by Rogers and Dalrymple needs to calculate the normal direction, which can cause additional difficulties for complex boundaries.

The dynamic SBT algorithm improves computational accuracy by removing the particle deficiency problem for fluid particles, and it is also suitable for complex solid boundaries. But in many cases, fluid particles may unphysically penetrate the solid walls. Also current algorithms for approximating field variable of the virtual particles are based on conventional SPH method, which is known to have poor accuracy. Conventional SBT algorithms with ghost particles are usually applicable only to simple or straightforward boundaries in order to generate ghost particles. The SBT algorithm by Marrone et al. is actually a combination of the dynamic SBT algorithm and the conventional SBT algorithms with ghost particles. Thus it can lead to comparatively better results. It should be noted that a second search is needed to locate the nearest neighbor particles for the image interpolation point, which may cause additional computational effort.

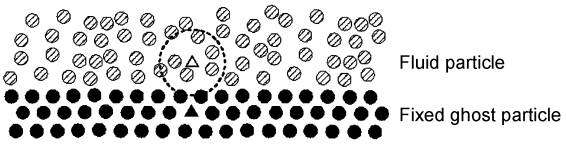

Figure 5 Illustration of the fixed ghost particle SBT algorithm by Marrone et al. [20].

4 A coupled dynamic SBT algorithm

Considering the advantages and disadvantages of the current boundary treatment methods, we propose a coupled dynamic SBT algorithm. In this new algorithm, two types of virtual particles, repulsive particles and ghost particles, are used (Figure 6). The repulsive particles are similar to the particles used in the repulsive SBT algorithms, and they are located right on the solid boundary. Ghost particles are located outside the solid boundary area. It should be noted that in conventional SBT algorithms, ghost particles are generated from mirroring or reflecting fluid particles onto solid boundary areas, and need to adapt to the fluid particles at each time step. In contrast, this new SBT algorithm can generate ghost particles in a regular or irregular distribution at the first time step, while ghost particle positions do not need to change during the following simulation.

The new SBT algorithm combines the advantages of repulsive SBT algorithms and dynamic SBT algorithms as a coupled approach. It is not a simple combination, as in this new SBT algorithm a new repulsive force for repulsive particles and a new interpolation scheme to approximate the information of the virtual particles have been proposed. The improved soft repulsive force can prevent unphysical particle penetration without obvious pressure disturbances as in repulsive SBT algorithms. The improved interpolation scheme serves to greatly improve the computational accuracy for calculating the information of the virtual particles.

The new repulsive force is an improvement on Kourosh's work [21], which needs to calculate the tangential and normal directions of solid boundaries and is not easy to implement for complex geometries. The improved repulsive force is a finite distance-dependent repulsive force on fluid particles approaching solid boundaries:

$$\boldsymbol{F}_{ij} = 0.01c^2 \cdot \chi \cdot f(\eta) \cdot \frac{\boldsymbol{x}_{ij}}{r_{ij}^2}, \tag{15}$$

$$\chi = \begin{cases} 1 - \dfrac{r_{ij}}{1.5\Delta d}, & 0 < r_{ij} < 1.5\Delta d, \\ 0, & \text{otherwise}, \end{cases} \tag{16}$$

$$\eta = r_{ij} / (0.75 h_{ij}), \tag{17}$$

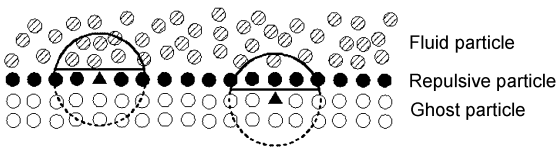

Figure 6 Illustration of the present coupled dynamic SBT algorithm.

$$f(\eta)=\begin{cases}2/3, & 0<\eta\leqslant 2/3,\\ (2\eta-1.5\eta^2), & 2/3<\eta\leqslant 1,\\ 0.5(2-\eta)^2, & 1<\eta<2,\\ 0, & \text{otherwise},\end{cases} \tag{18}$$

where Δd is the initial distance of two adjacent particles.

In this coupled dynamic SBT algorithm, the field variable of the virtual particles (both repulsive particles and ghost particles, see Figure 6) can be dynamically evolved and obtained from SPH approximation of neighbor fluid particles within the support domain. The interpolation domains of different kinds of virtual particles are different. The information of repulsive particles only comes from fluid particles, and the information of ghost particles comes from both fluid and repulsive particles. It is known that the support domains of the fluid particles intersect the solid boundary with insufficient neighbor particles for conventional SPH particle approximation schemes. Therefore, to restore the consistency of SPH particle approximation, Shepard filter method or moving least square (MLS) method can be used in the coupled dynamic SBT algorithm for approximating both the fluid and virtual particles.

Take non-slip boundary condition as an example. The variables of the boundary particles can be obtained from the following equations:

$$\rho_i^{\text{new}}=\sum_{j=1}^{N}\rho_j W_{ij}^{\text{new}}\frac{m_j}{\rho_j}=\sum_{j=1}^{N}m_j W_{ij}^{\text{new}}, \tag{19}$$

$$\boldsymbol{v}_i^{\text{new}}=-\sum_{j}^{N}\boldsymbol{v}_i W_{ij}{}^{\text{new}}\frac{m_j}{\rho_j}, \tag{20}$$

where $W_{ij}{}^{\text{new}}$ is the corrected kernel function, which represents the new function $W_{ij}{}^{\text{Shepard}}$ or $W_{ij}{}^{\text{MLS}}$ obtained by the Shepard filter or MLS method, respectively, and they can be written as

$$W_{ij}^{\text{Shepard}}=\frac{W_{ij}}{\sum_{j=1}^{N}W_{ij}\dfrac{m_j}{\rho_j}}, \tag{21}$$

$$W_{ij}^{\text{MLS}}=[\beta_0+\beta_x(x_i-x_j)+\beta_y(y_i-y_j)]W_{ij}, \tag{22}$$

$$\begin{bmatrix}\beta_0\\ \beta_x\\ \beta_y\end{bmatrix}=\left(\sum_{j=1}^{N}W_{ij}\boldsymbol{A}\frac{m_j}{\rho_j}\right)^{-1}\begin{bmatrix}1\\ 0\\ 0\end{bmatrix}, \tag{23}$$

$$\boldsymbol{A}=\begin{bmatrix}1 & x_i-x_j & y_i-y_j\\ x_i-x_j & (x_i-x_j)^2 & (x_i-x_j)(y_i-y_j)\\ y_i-y_j & (x_i-x_j)(y_i-y_j) & (y_i-y_j)^2\end{bmatrix}. \tag{24}$$

It has been demonstrated that improved SPH particle approximations with Shepard filter or moving least square correction can lead to much better results than conventional SPH particle approximation schemes [18]. This is different from the dynamic SBT algorithms which use conventional SPH approximations to obtain the information of virtual particles with comparatively much lower accuracy. It should be noted that existing modifications in SPH particle approximations with Shepard filter or moving least square are only used for approximating information of fluid particles. This is the first time to extend the idea to approximate information of virtual particles in treating solid boundaries.

5 Numerical examples

In this section, three numerical examples are presented to demonstrate the effectiveness of the coupling dynamic boundary algorithm. The first example involves dam break against a vertical wall (Figure 7), which is a classic dam break problem with a simple solid boundary. To examine its applicability to more complex boundaries, a sharp-edged obstacle is placed before the vertical wall during the dam breaking process (Figure 11). Finally, the water entry of a cylinder (Figure 14) is simulated to demonstrate the efficiency of the new algorithm in treating the moving boundaries.

5.1 Free dam break against a vertical wall

Free dam break against a vertical wall has been modeled using the SPH method by a number of researchers. Due to limitations in modeling solid boundaries, most researchers could only describe the problem qualitatively, such as flow pattern, water height and surge front. It is difficult to give precise prediction of the pressure load on solid boundary.

The geometry of this example is shown in Figure 7. In SPH simulation, around 30000 particles are used. Time step is taken as 0.00001 s, and the speed of sound is 40 m/s. Initial pressure field is given based on initial water height.

To validate the efficiencies of the coupled dynamic SBT algorithm, comparative analyses with other SBT algorithms are conducted. Figure 8 shows the particle and pressure distributions obtained from the repulsive force (a), dynamic (b),

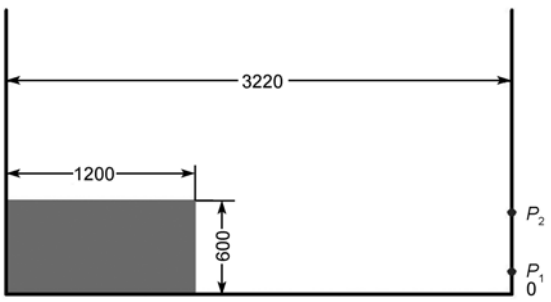

Figure 7 Numerical model of free dam break flow against a vertical wall (unit: mm).

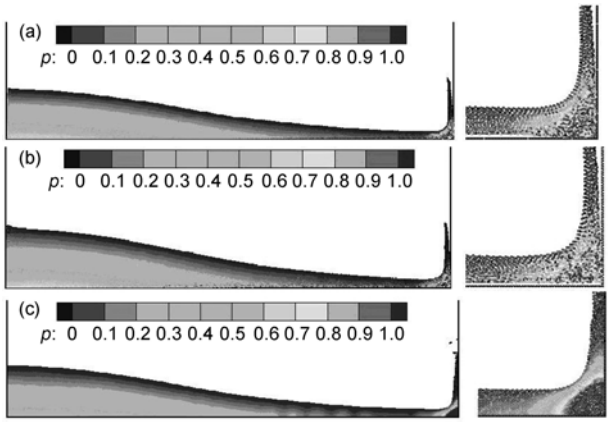

Figure 8 Particle and pressure distributions obtained using three SBT algorithms. (a) Repulsive force SBT; (b) dynamic SBT; (c) coupled dynamic SBT.

and coupled dynamic SBT algorithms. Three left figures show the whole flow pattern, and three right figures show zoom-in plots for the bottom-right corner area. It is obvious that repulsive force and dynamic SBT algorithms lead to rough pressure field with numerical oscillations especially in the bottom-right corner area. Also for both SBT algorithms, a clear particle separation can be observed near the top-right solid wall. It is therefore difficult to obtain accurate pressure loads on the solid boundary due to pressure oscillation and particle separation. In contrast, the pressure distribution obtained from the coupled dynamic SBT algorithm leads to more ordered particle distribution and much smoother pressure field which has clear pressure layers. Large impact pressure in the corner area can be effectively predicted with obvious pressure layers.

Figure 9 shows the flow history of the dam break problem at 0.3, 0.8, 1.4 1.6, 1.8, and 2.2 s. It can be observed that with the development of the dam-breaking process, water front impact against the front vertical wall generates a bounce-back flow pattern after interacting with the vertical wall, and finally forms a cavity in the bottom-right corner area. With repulsive force and dynamic SBT algorithms, no clear or smooth pressure has been obtained.

To quantitatively validate the pressure load on the solid boundary, two probe points P1, P2 are used (OP1 = 0.16 m, P1P2 = 0.424 m, as shown in Figure 7), and pressures obtained using the coupled dynamic SBT algorithm were compared with experiment observations by Buchner [22]. At approximately 0.6 s, water front impacts point P1, which generates a big pressure jump (approximately 0.65 times

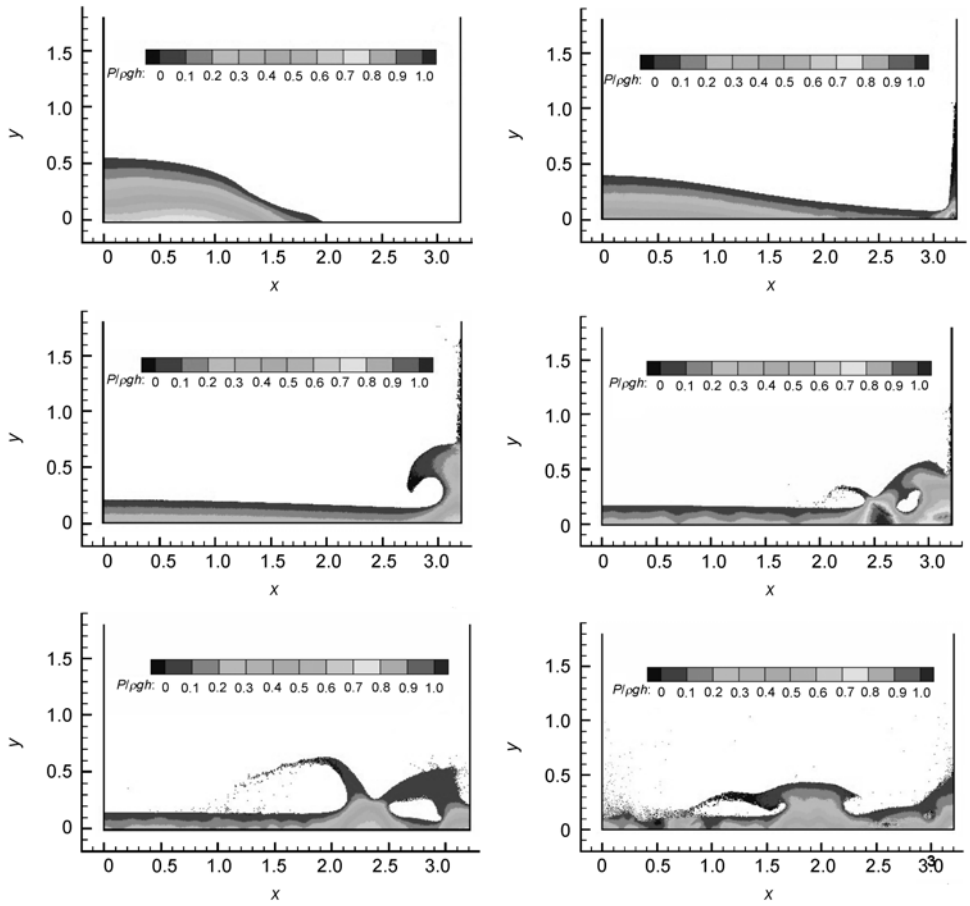

Figure 9 Pressure fields at 0.3, 0.8, 1.4, 1.6, 1.8, and 2.2 s for the dam break problem.

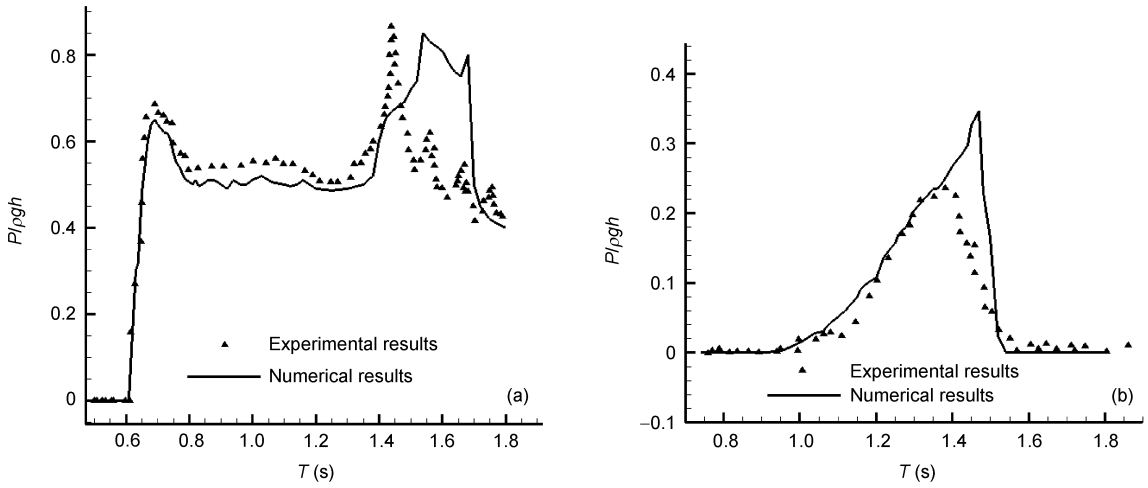

Figure 10 Comparison of experiment and numerical pressures at P1 (a), P2 (b).

the maximum hydrostatic pressure). From 0.6 to 1.4 s, pressure reduces. It is obvious that before 1.4 s, the numerical results agree well with experimental observations (Figure 10). While after 1.4 s, there exist bigger differences, largely due to the air entrapment (cavity) in the simulation. It is expected to obtain better agreement if using a two phase model (water and air) in the SPH simulation.

5.2 Free dam break against a sharp-edged obstacle

This example is similar to the above case except that a sharp-edged obstacle is placed before the right vertical wall, as shown in Figure 11. The sharp-edged obstacle can generate big water impact and it is difficult to precisely predict the pressure load. To track the value of the pressure, two probe points P1 and P2 are set in the sharp-edged obstacle, where OP2 = 2OP1 = 35.35 cm. The initial particle spacing is 0.01 m, about 20000 particles are used in the simulation, and the sound speed is 50 m/s.

Figure 12 shows the pressure evolution of the dam break against a sharp-edged obstacle. It is clear that when water front meets the sharp edge, a big pressure impact produces. After that, water particles spread away from the edge to generate a long strip of water. Most importantly, some particles splash away from the water strip and then fall onto the bulky water, leading to transient heavy pressure in some areas of the bulky water.

Using the conventional SPH method with previous SBT algorithms is not able to accurately resolve the pressure field near the sharp edge or near areas where splashed particles fall on the bulky water. It is easy to observe unphysical particles penetrations or big pressure oscillations with previous SBT algorithms. Again the coupled dynamic SBT algorithm can obtain smooth pressure field, well capture the spreading and formation of water strip. The flow patterns agree with those obtained by Colicchio [23] who simulated the case using Level-Set method. And the pressures on P1and P2 points are agreeable with the results by Marrone [19], with a 7% larger peak pressure in this coupled dynamic SBT algorithm. In Marrone's work, much more particles were used with much larger computational cost.

5.3 Water entry of a cylinder

Water entry phenomenon involves breakup of the free surfaces, fluid-solid interactions and complex turbulence and vortex generation, and therefore it is difficult for traditional numerical methods to simulate water entry problems. In this case, the water entry of a cylinder is simulated, and the coupled dynamic boundary algorithm is used in moving boundary. As shown in Figure 14, the length and height of the water are 200 and 50 cm, respectively, and the radius of the cylinder is 5.5 cm, which has the same density as water. The initial downward velocity of the cylinder is 2.955 m/s.

The objective of this example is to investigate the effectiveness of the new SBT algorithm with moving solid boundaries, and the pressure loads on moving objects. The initial particle spacing is 0.0025 m, about 160000 particles are used in the simulation.

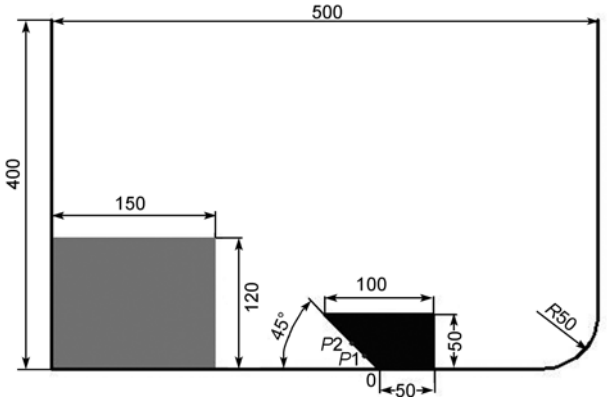

Figure 11 Numerical model of dam break flow against a sharp-edged obstacle (unit: cm).

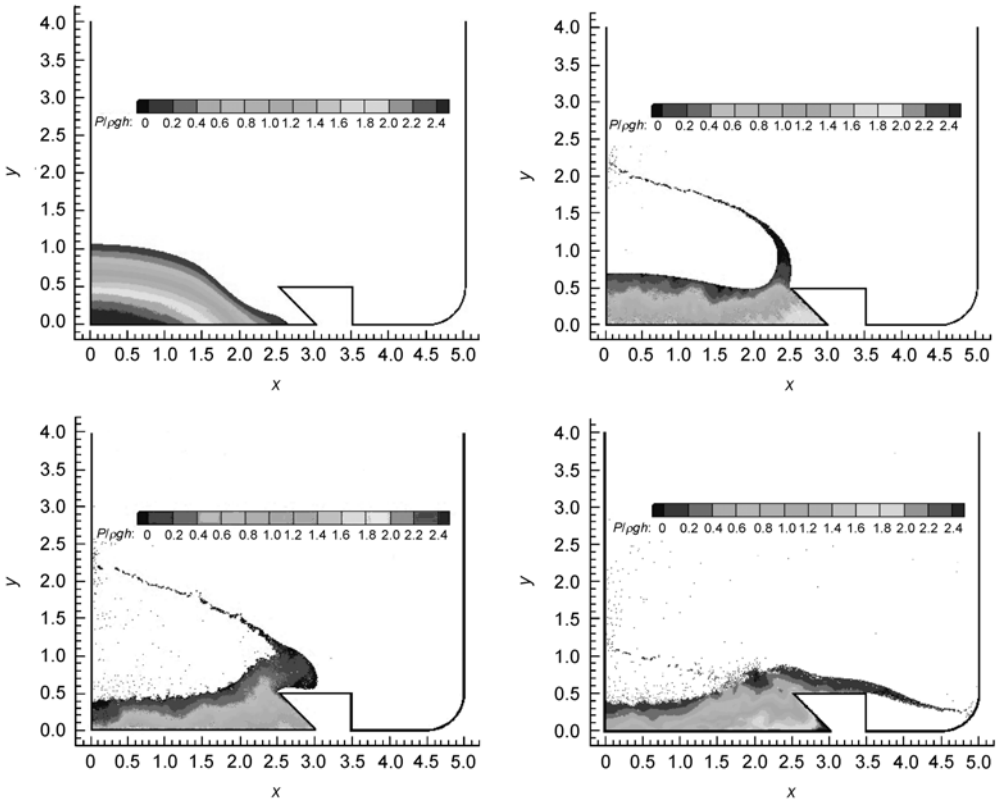

Figure 12 Pressure evolution at 0.37, 0.8, 1.31, 1.67 s of the dam break flow against a sharp-edged obstacle.

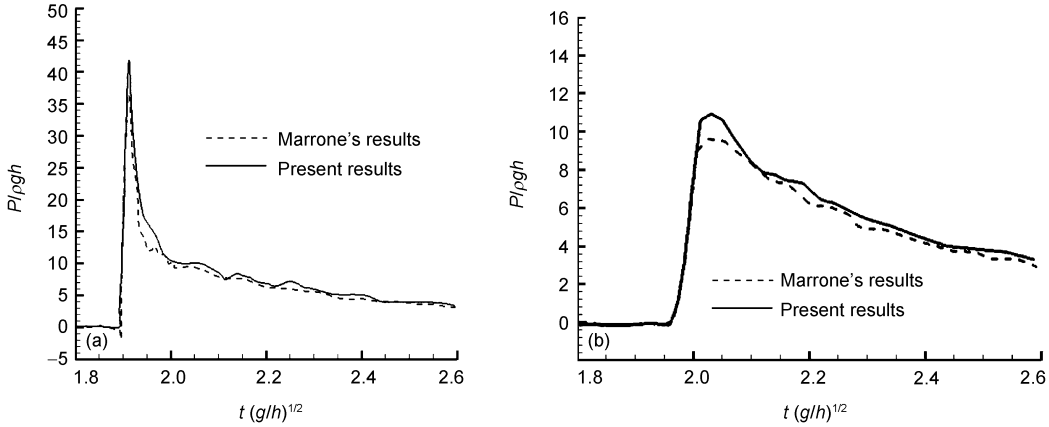

Figure 13 Comparison of pressures at P1(a) and P2(b) with two SBT algorithms.

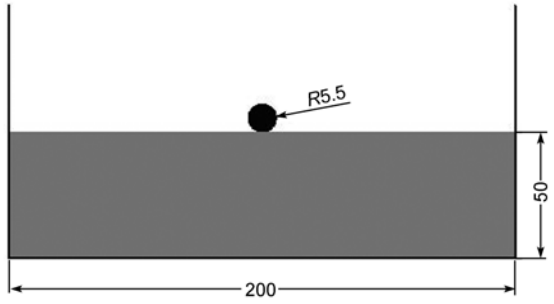

Figure 14 Numerical model of the water entry of a cylinder (unit: cm).

Figure 15 shows the pressure evolution during the water entry process at 0.006, 0.02, 0.03, 0.035, 0.2, 0.26 s. At 0.006 s when the cylinder meets the water surface, a pressure wave produces and then transmits in water. At 0.02 s, after the interaction with the solid wall, the pressure wave changes its direction and forms a reflection wave with a maximum pressure of about 12000 Pa. The whole pressure field is smooth during the pressure wave propagation. The reflection wave meets the falling cylinder at about 0.03 s, and produces a new interaction with the cylinder. With these disturbances, the pressure field is not as smooth as

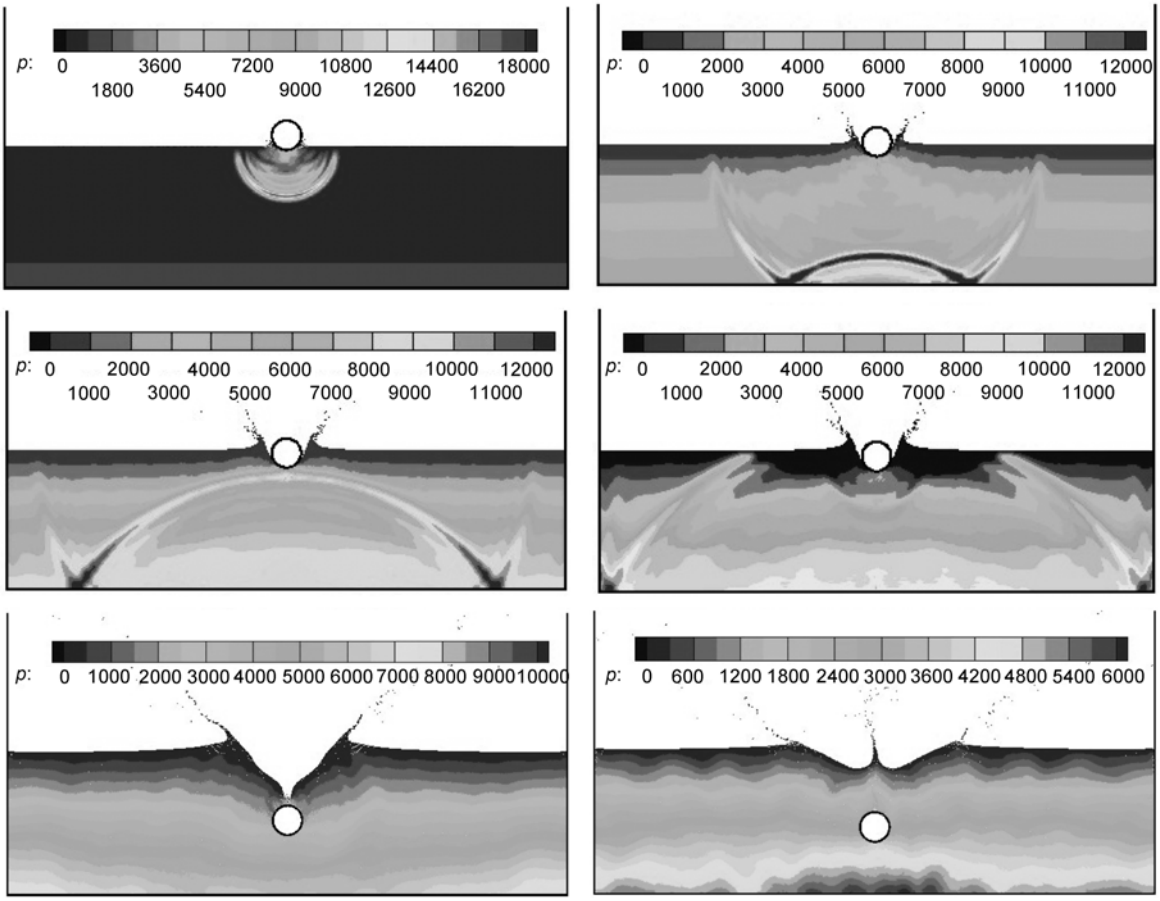

Figure 15 Pressure evolution at 0.006, 0.02, 0.03, 0.035, 0.2, 0.26 s.

before. However, this effect will gradually disappear as time elapses and the pressure field becomes smooth again.

Figure 16 shows the experimental observations by Greenhow [24] and SPH results with coupled dynamic SBT algorithm. It is clear that the obtained SPH results are close to experimental observations, and it shows that this coupled dynamic SBT algorithm is also effective for moving solid boundaries.

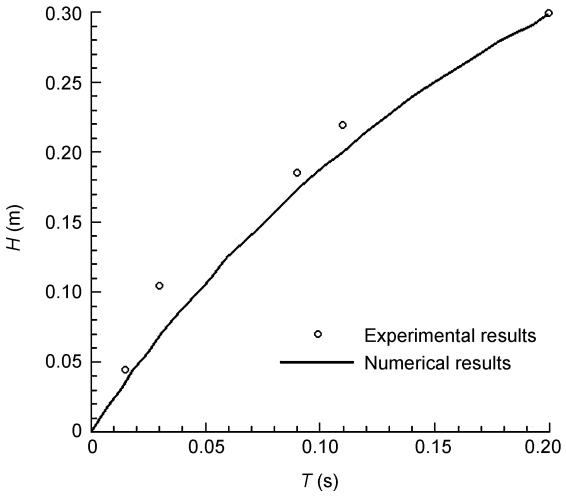

Figure 16 Penetration depths obtained from numerical simulation and experimental observation.

6 Conclusions

This paper presented a coupled dynamic algorithm for treating solid boundaries in the SPH method. Solid boundaries and obstacle areas are represented by virtual particles including repulsive particles located right on the solid boundaries, and ghost particles in the obstacle areas. A new repulsive force for repulsive particles and a new interpolation scheme to approximate the information of the virtual particles have been proposed, which can prevent unphysical penetration of flow particles through solid boundaries, and improve the computational accuracy respectively. The effectiveness of the new solid boundary treatment algorithm has been demonstrated by three numerical examples with better accuracy and smoother pressure field.

This work was supported by the National Natural Science Foundation of China (Grant Nos. 10942004, 11172306) and the National Defense Innovation Funds of the Chinese Academy of Sciences (Grant No. Y175031XML).

1 Gingold R A, Monaghan J J. Smoothed particle hydrodynamics-theory and application to non-spherical stars. Mon Notic Roy Astron Soc, 1977, 181: 375–389
2 Liu M B, Liu G R. Smoothed particle hydrodynamics (SPH): An overview and recent developments. Arch Comput Method Eng, 2010, 17(1): 25–76
3 Liu M B, Liu G R, Lam K. Constructing smoothing functions in smoothed particle hydrodynamics with applications. J Comput Appl Math, 2003, 155(2): 263–284
4 Monaghan J J. Smoothed particle hydrodynamics. Rep Progr Phys, 2005, 68(8): 1703–1759
5 Frenkel D, Smit B. Understanding molecular simulation: From algorithms to applications. Adv Veter Med Ap, New York, 2002
6 Hoogerbrugge P J, Koelman J. Simulating microscopic hydrodynamic phenomena with dissipative particle dynamics. Europhys Lett, 1992, 19: 155
7 Li S, Liu W K. Meshfree and particle methods and their applications. Appl Mech Rev, 2002, 55(1): 1–34
8 Nguyen V P, Rabczuk T, Bordas S, et al. Meshless methods: a review and computer implementation aspects. Math Comput Simulat, 2008, 79(3): 763–813
9 Monaghan J J. Simulating free surface flows with SPH. J Comput Phys, 1994, 110: 399–399
10 Morris J P, Fox P J, Zhu Y. Modeling low Reynolds number incompressible flows using SPH. J Comput Phys, 1997, 136(1): 214–226
11 Liu G R, Liu M B. Smoothed particle hydrodynamics: A meshfree particle method. World Scientific Pub Co Inc., 2003
12 Yang X F, Peng S L. Simulation of dam-break flow with SPH method. China J Comput Phys, 2010, 27(2): 173–180
13 Monaghan J J. Simulating free-surface flows with SPH. J Comput Phys, 1994, 110(2): 399–406
14 Rogers B, Dalrymple R. SPH modeling of tsunami waves. Adv Num Model Simul Tsun Wave Runup, 2007. 75–101
15 Gomez-Gesteira M, Dalrymple R A. Using a three-dimensional smoothed particle hydrodynamics method for wave impact on a tall structure. J Water Port Coast Oc Asce, 2004, 130(2): 63–69
16 Gong K, Liu H. Water entry of a wedge based on SPH model with an improved boundary treatment. J Hydrodyn Ser B, 2009, 21(6): 750–757
17 Libersky L D, Petschek A G. High-strain Lagrangian hydrodynamics—a 3-dimensional SPH code for dynamic material response. J Comput Phys, 1993, 109(1): 67–75
18 Colagrossi A, Landrini M. Numerical simulation of interfacial flows by smoothed particle hydrodynamics. J Comput Phys, 2003, 191(2): 448–475
19 Marrone S, Colagrossi A. Delta SPH model for simulating violent impact flows. Comput Method Appl Mech Eng, 2010. 1526–1542
20 Fries T, Matthies H. Classification and overview of meshfree methods. Tech Univ Braunschweig, 2003
21 Kourosh A. SPH simulation of hydrodynamic forces on subsea pipelines. Personal Communication, 2010
22 Buchner B. Green Water on Ship-type Offshore Structures. PhD Thesis. Delft: Delft University of Technology, 2002
23 Colicchio G. Violent Disturbance and Fragmentation of Free Surfaces. PhD Thesis. Southampton: University of Southampton, 2004
24 Greenhow M, Lin W M. Nonlinear free surface effects: Experiments and theory. Depart Ocean Eng, 1983, Report No. 83-19